Identifying key parameters through a sensitivity analysis for realistic hygrothermal simulations at wall level supported by monitored data.

Simone Panico[1,2,*], Marco Larcher[1], Valentina Marincioni[3], Alexandra Troi[1], Cristina Baglivo[2], Paolo Maria Congedo[2]

[1] Institute for Renewable Energies, Eurac Research, Viale Druso 1, 39100 Bolzano, Italy
[2] Department of Engineering for Innovation, University of Salento, 73100 Lecce, Italy
[3] UCL Institute for Environmental Design and Engineering, 14 Upper Woburn Place, WC1H 0NN, London, United Kingdom
* Correspondence: simone.panico@eurac.edu

HIGHLIGHTS

- Assessing the reliability of hygrothermal simulations.
- Description of monitoring conducted in a historic building.
- Calibration of the model compared to monitoring data.
- Validation of the numerical model.
- Sensitivity analysis of materials parameters and boundary condition coefficients.

ABSTRACT

The reliability of hygrothermal simulations of building components is key for designing energy efficiency measures, assessing living comfort, and preventing building damage. The model accuracy is related to the reliability of the selection of input parameters. Due to the high uncertainty, the selection of the input values is challenging. This work aims to calibrate a hygrothermal simulation model exploiting monitored values recorded in a case study located in Settequerce (Italy), to understand how close to reality a numerical model can be. Moreover, a sensitivity analysis, based on the Morris method together with a Latin Hypercube sampling, is applied to identify the input parameters that affect most significantly the simulation. The results of the calibration indicated that is possible to obtain reliable outputs by appropriately selecting materials within the database. The sensitivity analysis showed that the relative humidity under the insulation is largely influenced by the water vapor diffusion resistance factor of the plaster, applied during the renovation phase both on the internal and external side. Among the coefficients describing the coupling with the boundary conditions, only the external convective heat coefficient and the coefficient of short-wave solar radiation influence slightly the objective function.

KEYWORDS

- Hygrothermal simulation
- Monitoring
- Calibration
- Validation
- Sensitivity Analysis

1 Introduction

When planning a historic building renovation, a common solution is to apply internal wall insulation to preserve the aesthetic appearance and heritage value of the external façade [1]. The application of insulation from the inside is a practice used to safeguard the historic exterior surfaces but at the same time, it reduces the heat flow from the occupied rooms to the historic wall, making it colder. This increases the risk of interstitial condensation and moisture related damages [2]. The moisture accumulation within the insulated wall can damage the envelope and, in case of mold growth, the health of the occupants. For this reason, it is necessary

to carefully plan an intervention using the right tools. Among those, hygrothermal simulations are a valuable tool for researchers and designers.

Nowadays, it is possible to use numerical models to simulate and predict masonry conditions before and after the intervention. Despite this, the construction of the numerical model can be complex; it requires knowledge of a large number of input parameters that are often not easy to obtain. Furthermore, the numerous uncertainties complicate the relationship between the model's inputs and outputs, increasing the complexity [3]. Therefore, a stochastic model has been used [4] by taking uncertainties into account in the numerical model, leading to longer calculation times. On the other hand, as computing power increases, the performance of building performance simulations improves [5].

Hens [6] stated that it is unrealistic to claim a perfect agreement between model and reality. However, numerical models can aim to predict the hygrothermal conditions in building components [7]. In the case of hygrothermal simulations, the complexity of the physical phenomena involved makes it difficult to represent the simulated model. For example, most building materials are hygroscopic and can contain moisture in different thermodynamic phases [8] which change their hygrothermal response. This is certainly relevant for historic masonry buildings, which are notoriously difficult to replicate in hygrothermal models [9]. Although climate data are frequently averaged or based on empirical coefficients, they do not always correspond to the actual design conditions. In the case of materials, the identification of the correct input parameters can be difficult, especially when dealing with historical walls which are formed by a combination of materials (stones and mortar joints) whose hygrothermal properties are typically unknown [10].

For those reasons, uncertainties must be accepted, and, to avoid making design mistakes, the results must be carefully interpreted. At the same time, the greater the level of knowledge of the input parameters, the greater the probability that the model will return reliable outputs [11]. For this reason, a good strategy is to make an effort to minimize input parameter uncertainty. In particular, a good knowledge of the parameters of the materials constituting the walls is essential for a good agreement between the simulated and the real values [12].

How accurately a hygrothermal simulation model represents reality is still a matter of debate today. Numerous studies have investigated how accurate simulation software can be [13–15]. Several studies have tried to calibrate hygrothermal simulations [16–23]. Calibrating a model that describes only heat transport is already challenging [24,25], whereas, when it comes to the hygrometric part, there is a greater number of parameters that need to be considered [26]. In the literature, numerical model calibration is often carried out using laboratory scale samples [19,22,27]. In particular, sometimes the calibration has been performed by varying input parameters or, in other studies, the model outputs have been evaluated by choosing different materials. For example, in work carried out by Jensen, N et al. [2], the calibration of the numerical model was carried out against values of the relative humidity recorded within the wall, evaluating the effects on the output by changing the type of mortar and the effect of varying the thicknesses of materials in the numerical model. Hansen, T et al. [28] investigated the impact of varying specific parameters on the relative humidity results in three points within a brick masonry. A stochastic approach is conducted by [29–31] in which model outputs consider the uncertainties of the inputs. To date, there is a lack of guidelines for calibrating hygrothermal models [25]. No works in the literature consider calibrations and validations of hygrothermal models using long-term monitoring data in actual buildings [25] using values monitored inside the building component.

Input parameter measurements, such as those for the climate or the materials, can in any case significantly decrease the model's uncertainty [7]. However, these measures are frequently time-consuming and costly. Nevertheless, they are still the best support for reducing uncertainties, but such measures should be guided and limited to only those parameters which would most improve the reliability of the hygrothermal simulation.

The application of a sensitivity analysis to the numerical model can yield crucial information that allows for the identification of the most influential parameters and, consequently, indicate which input parameters should be investigated to significantly reduce the uncertainties of the hygrothermal simulation [32,33]. Zhao et al. [31] proposed a probabilistic method by evaluating the most influential parameter with respect to the thermal

resistance of the wall. Marincioni et al. [34], developed a methodology that aims to create a probabilistic predictive model for the assessment of moisture risks considering model uncertainties. T. Valdbjørn et al. [33] applied sensitivity analysis with the Morris method and the Sobol method to find parameters that are negligible among insulation thickness and conductivity, vapor barrier, wall orientation, air-change rate, and driving rain. The parameters are varied using a uniform distribution. The sensitivity analysis is performed to the innermost and outmost layer of a brick wall, in order to evaluate the average moisture content. In particular, P. Heiselberg et al. [35] provided a complete overview of the types of sensitivity analysis, pointing out the advantages of the Morris Method which is evaluated as the most interesting for sensitivity analysis in sustainable building design.

This paper echoes what has been carried out by Zhao et al. [31] and Marincioni et al. [34] by comparing hygrothermal simulation results with monitoring data collected in a renovated historic wall insulated from the inside. The monitoring data refer to a very long period of almost 2 years and include the hygrothermal conditions occurring in the wall during both hot and cold periods. The innovative methodology uses those long-term monitored data to calibrate and validate a hygrothermal simulation model; moreover, they are also used to perform a sensitivity analysis. This research focuses on two open questions. First, an analysis is conducted to determine how realistic the hygrothermal simulation model can be when applied in the context of the interior insulation of a historic stone masonry wall. Subsequently, in the second step, a sensitivity analysis method is used to identify the input parameters that most influence the numerical model. In particular, this is an essential aspect as the literature lacks a study of how different material properties influence the final results of a hygrothermal simulation [33]. Finally, a validation of the calibrated model verifies its robustness.

2 Methodology

This section outlines all steps of study development. . A hygrothermal analysis software is used to simulate a masonry wall of a historic building. In particular, Delphin 6.1 software is used. The creation of the model involves recreating the cross-section of the wall, assigning the material, the environmental conditions (internal and external), and the initial conditions of the component. The wall model is created based on the material thicknesses measured on site. The model is supplied with data from the monitoring system that measures the external climate conditions (described in **Section 2.1**) and those in the indoor room. In this way, it is possible to minimize the uncertainties related to the climatic conditions the wall is subjected to. The numerical model simulates the behaviour of the walls over the entire monitored period. The simulation outputs have been set to coincide with the temperature and relative humidity values at the same points in the cross-section where the sensors are installed. This allowed a comparison between the values obtained from the simulation and those recorded during the entire monitoring period. **Table 1** shows all input parameters used in this study and the variables considered for model calibration and sensitivity analysis.

Input Parameters		Type of input data	Sources used for the calibration	Sources used for the sensitivity analysis
External climatic conditions	Temperature	Hourly data [°C]	Data from monitoring System	Data from monitoring System
	Relative Humidity	Hourly data [%]	Data from monitoring System	Data from monitoring System
	Short Wave Solar Radiation	Hourly data [W/m^2]	Data from monitoring System	Data from monitoring System
	Direct rain on surface	Hourly data [l/m^2]	Data from monitoring System	Data from monitoring System
Indoor climatic conditions	Temperature	Hourly data [°C]	Data from monitoring System	Data from monitoring System
	Relative Humidity	Hourly data [%]	Data from monitoring System	Data from monitoring System
Materials properties	Thermal transport	Thermal conductivity as function of moisture content	Parameter Variation: Section 2.4 (Model Calibration)	Parameter Variation: Section 2.5 (Sensitivity analysis)
	Thermal storage	Thermal storage parameters		
	Vapor transport	Vapor permeability as function of moisture content		
	Liquid transport	Liquid conductivity as function of moisture content		

	Moisture storage	Moisture content as function of capillary pressure		
Boundary coefficients	Heat conduction	Exchange coefficient [W/m²k]	Fixed value: WTA Recommendations 6.2 [36]	Parameter Variation: Section 2.5 (Sensitivity analysis)
	Vapor diffusion	Exchange coefficient [s/m]	Fixed value: WTA Recommendations 6.2 [36]	
	Short wave radiation	Absorption coefficient of the building surface [-]	Fixed value: DIN 18599 [37]	
	Wind-driven rain	Rain exposure coefficient [-]	Fixed value: EN 15927-3 [38]	

Table 1. All input parameters used to create the numerical model. The cells in green indicate the sources from which the values are taken. Cells in yellow indicate the input parameters varied for calibration and sensitivity analysis.

After implementing the numerical model, the next step concerns the analysis and evaluation of uncertainties. Since the boundary conditions are monitored, the most significant uncertainties are associated with the choice of materials in the model. The knowledge of the materials changes depending on whether the material is new (i.e., a material added during the building renovation) or existing. Therefore, it is essential to create a cluster of materials selected from the software database that is representative of each material present in the wall cross-section. **Section 2.3** describes in detail the selection of clusters for each material. The implemented procedure exploits the clusters for the calibration of the numerical model: a *Python* script combined with the simulation tool ran several simulations using different combinations of materials to find the one that minimized the difference between the simulated and monitored data indicated as objective function (**Section 2.4**). Afterward, the calibrated model is validated over a later period. Finally, a sensitivity analysis is performed using the calibrated simulation, to determine the input parameters most influencing a selected objective function. The sensibility model used is discussed in more detail in **Section 2.5**.

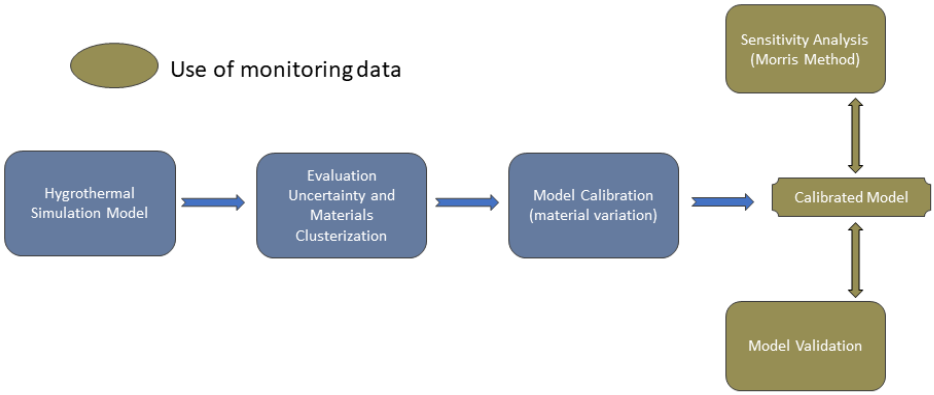

Figure 1. Applied framework to find a calibrated model, conduct sensitivity analysis and finally validate the model.

2.1 Case Study

A monitoring system was installed in a historic building located in Settequerce (Bolzano – Italy). The building was retrofitted in 2017 and a wood fiber insulation panel was applied from the internal side on the exterior stone walls. Sensors were installed on the external and internal surfaces, as well as within the wall, during the renovation, as shown in **Figure 2**. Detailed information on the monitoring system can be found in [23,24].

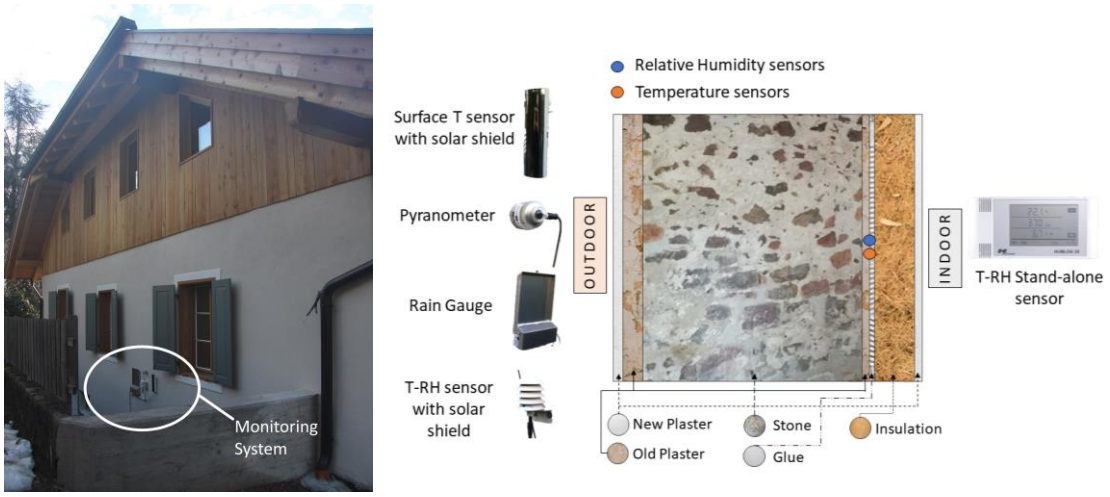

Figure 2. Cross-section of the analyzed masonry (left), the wall analyzed and all sensors placed on the external surface (right)

On the outside, a pyranometer (Hukseflux SR05), a driving rain gauge (SMT – RS1119), a surface temperature sensor (thermocouples), and a temperature and humidity sensor (E + E EE060) were installed. The external temperature sensors were shielded to prevent solar radiation from affecting their measurements [39]. On the inside, a stand-alone sensor (E+E HUMLOG) for temperature and relative humidity was placed in the room. Temperature and relative humidity sensors (E + E EE060) were also installed within the wall during the renovation phase in the locations represented in **Figure 2**. To increase the measurement reliability, two sensors were placed in the layer behind the insulation. The sensing elements of the sensors were shielded to protect them from dirt, dust, chemicals, and salts. The sensors are linked to an external acquisition station, which houses a computer and a device that gathers all the recorded data. Data collection started in February 2017. The data used in this work refer to 22 months of data logging.

Figure 3 shows the temperature and relative humidity values used as input boundary conditions of the numerical model. The values of the heat coupling coefficients h_{int} and h_{ext} and of the vapor exchange coefficients β_{int} and β_{ext} are selected following the WTA 6.2 guidelines [36]. The coupling parameters h_{int} and h_{ext} are assigned the values 8 $\frac{W}{m^2K}$ and 17 $\frac{W}{m^2K}$, respectively. For β_{int} and β_{ext}, the values 2.5 x 10^{-8} $\frac{s}{m}$ and 7.5 x 10^{-8} $\frac{s}{m}$ are used, respectively.

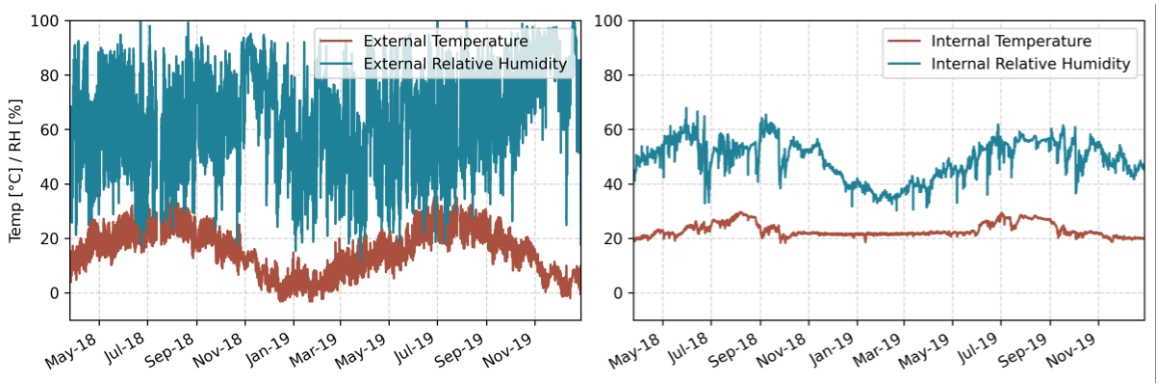

Figure 3. Temperature and relative humidity values recorded by the monitoring system with the internal HUMLOG sensor (left) and the external E+E sensor (right).

The solar radiation absorption coefficient is chosen based on the standard DIN 18599 [37]. Since the surface plaster is white, the value 0.4 is assigned to build the numerical model. The rain values are calculated

according to the model described in ISO 15927 [38]. Therefore, the rain exposure coefficient editable in Delphin is set to the value 1. The graph in **Figure 4** shows the recorded solar radiation and the driving rain on the North-east wall (62° North) for the entire observation period used as input boundary condition for the numerical model.

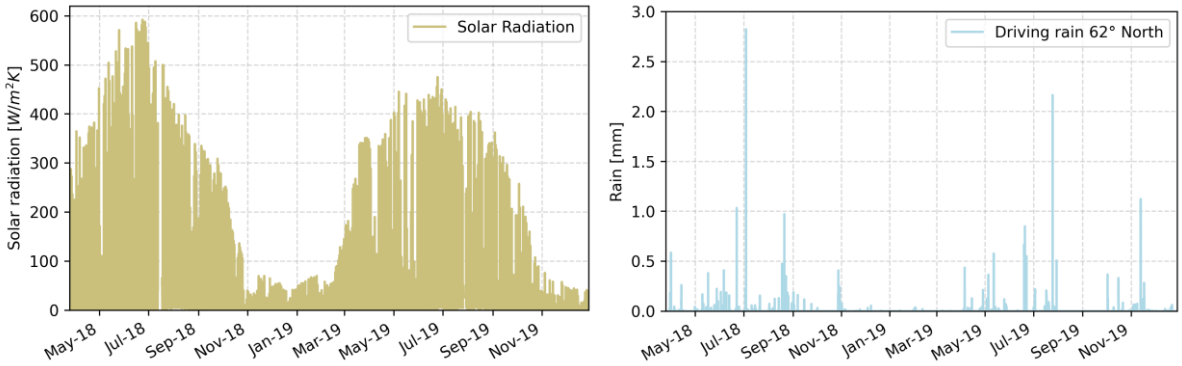

Figure 4. Solar radiation and rain values recorded by the monitoring system from the external pyranometer (left) and the driving rain gauge (right).

2.2 Description of the Numerical Model

This paper uses the hygrothermal simulation software Delphin, developed at the Technical University of Dresden[40].

Delphin allows the calculation of the coupled transport of heat and moisture to be simulated in 1-D, 2-D, and 3-D. Modelling involves describing the flow using physical models between volume elements (including material interfaces) and at the boundaries (external or internal interfaces). The flow is described by a set of balance equations. The numerical solution is obtained by a semi-discretization in space (using a finite volume/control method) and a subsequent integration in time. The model then converts the integral performed on the surface into the sum of the flux on all surfaces. The calculation of the flux into the volume performed on each representative elementary volume (REV) must be equal to the flux out of the volume. The procedure for estimating the flux divergence is applied iteratively to achieve convergence for the current time step. Below are the equations used in the numerical model to describe moisture and heat transfer.

Convective liquid (capillary) water flux:

$$j_{conv}^{m_l} = -K_l(\theta_l)[\frac{\partial p_l}{\partial x} + \rho_l g] \qquad \textit{Eq. 1}$$

Diffusive water vapor flux: :

$$j_{diff}^{m_v} = -\frac{D_{v,air}}{\mu * R_v * T}\frac{\partial p_v}{\partial x_k} \qquad \textit{Eq. 2}$$

***Heat conduction flux*:**

$$j_{diff}^{Q} = -\lambda(\theta_l)\left[\frac{\partial T}{\partial x_k}\right] \qquad \textit{Eq. 3}$$

Where subscripts *l* and *v* denote liquid and vapor respectively, while *conv* and *diff* involve convective and diffusive transport. The other parameters are described in the nomenclature table. For more details on the equations and for the description of the models for the coupling with the boundary conditions, the reader can refer to the *Delphin* software manual [41].

2.3 Material Clustering

It is generally recognized that simulation software is essential for hygrothermal assessment. Simulations must be carried out carefully because – particularly in the case of a historic building – the numerous uncertainties

can adversely affect the accuracy of the results. Therefore, it is reasonable to assume that better quality in the input parameters will return a more accurate simulation. External climatic data, such as temperature and relative humidity, solar radiation and driving rain, and the internal parameters (temperature and relative humidity), are important and must be chosen carefully. The material characteristics of all components are further essential inputs to the model. For this study, the climatic conditions are assumed to be correct since they are measured by the monitoring system. More attention is therefore paid to the selection of the input related to the materials.

The materials used in the numerical model are supposed to be as close as possible to those present in the investigated wall. Material selection is a challenging task, especially when dealing with historical materials. In this phase, clusters of material files have been created, selecting them from the database of the software Delphin 6.1. Every material will be afterward assigned to the corresponding layer in the cross-section of the numerical model to identify the best combination by comparing the outcomes with the monitoring data. To obtain adequate results for the sensitivity analysis study, the materials selected have to be representative of those found in the cross-section. At the same time, considering a greater variability of materials with different properties in every cluster allows a greater number of possible solutions to be investigated. The selection of materials can vary greatly depending on the level of knowledge available in the specific case study (documentation, laboratory tests, or historical materials with unknown properties). Only materials equivalent to the actual present in the cross-section are taken into consideration to prevent finding an unrepresentative combination.

A knowledge level that only considers the type of material found in the wall is used in this study. The following characteristics of the five materials that compose the investigated wall are taken into account when creating the clusters:

- The plaster applied to exterior and interior surfaces is a lime-based plaster. Therefore, all lime plasters are considered for this cluster.
- The glue used to adhere the insulation to the historic wall is a clay-based glue. Since there are only a few clay glues in the database, other glue types are also considered in order to have greater variability.
- A wood fibre-based insulation has been installed. Material is found in the database with very similar characteristics to those reported in its datasheet. However, all wood-fibre-based insulation materials are considered for the creation of the cluster.
- Since the composition of the historical plaster in the cross-section is unknown, all plasters in the database are considered. In this way, the great uncertainty regarding the properties of this material is taken into account.
- The historic stone in the wall consists of stone blocks bonded together with a historic mortar. Impurities from construction and possible voids are also present in this layer. For these reasons, all natural stones in the database have been considered to take uncertainties into account (excluding some materials such as tuffs and marbles to avoid including unrepresentative materials).

2.4 Model Calibration

This section describes the methodology used to calibrate the numerical model. The calibrated model aims to approach the relative humidity and temperature values under the insulation obtained as an output from the simulation with those recorded by the sensors at the same location. The sensors installed behind the insulation play an important role in this study. Indeed, the temperature and relative humidity sensors placed in the cross-section are used as a benchmark compared to the output obtained from the simulation. The statistical index (χ^2) is calculated to summarize how close the model is to the monitored values. This index is a modified RMSE (Root Mean Square Error) that accounts for measurement uncertainty.

$$\chi^2_{\mathrm{T}} = \frac{1}{N}\sum_i \left(\frac{T_{i,mon} - T_{i,sim}}{e_{T_{i,mon}}} \right)^2 \quad \text{Eq. 4}$$

$$\chi^2_{\mathrm{RH}} = \frac{1}{N}\sum_i \left(\frac{RH_{i,mon} - RH_{i,sim}}{e_{RH_{i,mon}}} \right)^2 \quad \text{Eq. 5}$$

Where:

- $T_{i,mon}$ and $RH_{i,mon}$ indicate the temperature and the relative humidity recorded by the sensors.
- $T_{i,sim}$ and $RH_{i,sim}$ indicate the hourly outcome in terms of temperature and relative humidity obtained with the hygrothermal simulation.
- $e_{T_{i,mon}}$ and $e_{RH_{i,mon}}$ represent the measurement uncertainty calculated as the maximum value between the sensor's accuracy (± 0.3 °C and 0.5 %) and the standard deviation between the two sensors placed behind the insulation.

A low index value indicates that the simulation is very close to the observed data. A value between 0 and 1 corresponds to a simulation output that falls within the uncertainty. In this specific paper, the values obtained from the sensors positioned under the insulation ($\chi^2_{avg,bi} = \frac{\chi^2_{RH,bi} + \chi^2_{T,bi}}{2}$) are considered as objective function. This position is considered because it is the most critical point from a hygrothermal point of view. Indeed, moisture accumulation is likely to occur, which can lead to interstitial condensation. In order to have a comparison index for validation, the MAE (*mean absolute error*) and RMSE (*root mean square error*) are also calculated. According to [42,43] this index is useful for the calibration of an energy model. Of the criteria listed in [21], a value of MAE and RMSE < 1°C for temperature and < 5% is an adequate value for the validation of a calibrated model. The proposed method involves a parameter variation (one at a time) of the materials in the database grouped in clusters for each type. That makes it possible to identify the best combination.

Since running all possible combinations would have been costly in terms of simulation time, the following approach is proposed. First, five materials $A - B - C - D - E$ (taken from each respective cluster) are assigned to the model. Then a *Python* script is implemented to vary the assigned materials (one by one), run the simulation, and calculate the $\chi^2_{avg,bi}$ index. The script proceeds as follows: four materials are fixed while the fifth is varied by assigning a material present in the corresponding cluster. After varying all the materials, the one that minimizes the index is identified and "fixed". The script then continues, varying a second material (of the four originally considered fixed) and again identifies the material with the lowest index and fixes it again. This procedure continues until all materials have been varied and then fixed. To consider a more significant number of possible combinations, the order in which the materials are varied is also changed. For example, consider the materials with the letters $A - B - C - D - E$ that were originally assigned to the model. First, the material A is varied to obtain A_{best}. Then it is fixed: $A_{best} - B - C - D - E$. Then B is varied and $A_{best} - B_{best} - C - D - E$ is obtained. And so on until the five "best materials of the first iteration are obtained: $A_{best} - B_{best} - C_{best} - D_{best} - E_{best}$.

This permutation method considers all possible combinations. In the second iteration, the order of the variations is, for example: $A - B - C - E - D$, then $A - B - D - C - E$ and so on. This results in 120 different orders in which the five materials are varied. This allows a greater variety of combinations, resulting in a more accurate identification of the materials that produce the best agreement with the monitored data.

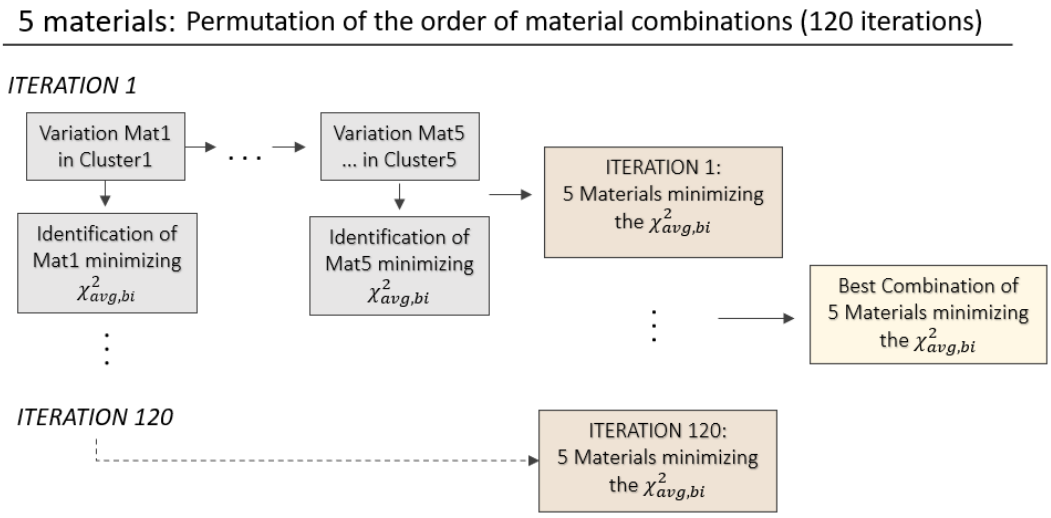

Figure 5. Process of identifying the best combination of materials against the monitored data.

2.5 Sensitivity Analysis

Sensitivity analysis is defined as the study of how the uncertainty in the output of a model (numerical or otherwise) can be apportioned to different sources of uncertainty in the model input [44]. The variation of parameters and functions in the respective plausibility ranges is carried out considering all materials in each cluster and the coefficients of coupling with the boundary conditions. The objective is to identify the input parameters that are more important in the simulation. A screening method (Morris's method) is implemented for this analysis, which allows a large number of variables to be considered but at the same time runs a relatively small number of simulations. The following paragraphs describe the sensitivity analysis method adopted, the input parameters considered and how their variation is handled within the numerical model.

2.5.1 Morris Method

The Morris method aims at identifying the impact of parameters on a defined objective function when the number of uncertainty factors is high and with a relatively small number of simulations [45]. It represents a screening strategy that considers non-monotonic relationships and information on the interaction of parameters. The Method has been developed by Morris (1991). Campolongo [46] proposes an improved version of the sampling approach [47] and the use of a radial design as a sensitivity analysis model.

The method is classified as OAT (one at a time), and it entails varying one input parameter at a time while keeping all others constant (at a random value) and calculating the variation of the objective function. The results provide a qualitative view of the parameters that matter most and recognize the inter-dependencies between them.

The sampling phase is performed using Latin Hypercube Sampling (LHS) [48]. The identified clusters referred to each material are used to extract the discrete distribution and then for sampling. A further step is to assign a probability density function to each parameter. A *Python* script (*SciPy* library) creates several distribution curves (Uniform, Gamma, Normal and Pareto distribution) for each discrete distribution of any given parameter. The Sum of Square Error (SSE) is then calculated, and the distribution that minimizes the SSE value is identified. This way, the discrete distributions are fitted to obtain the best approximated continuous distribution. The LHS is chosen to perform random sampling from probability distributions for each parameter. This methodology allows the generation of random numbers covering the entire input space. In addition, this sampling method uses stratified sampling to reduce the sample size but still accurately represents the probability density function (pdf). An example of the distribution obtained is shown in **Figure 6**. The discrete values of the λ_{dry} parameter

extracted from the cluster referring to the Old Plaster are compared with those sampled with LHS method using the best distribution obtained.

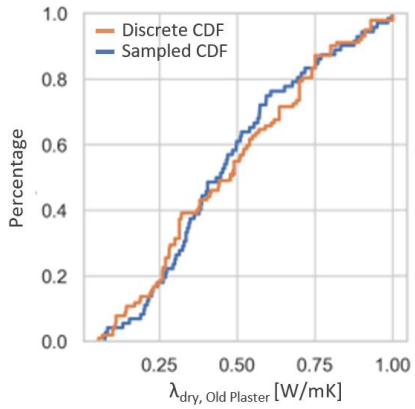

Figure 6. Comparison of the sampling by LHS method using the best distributions (among Uniform, Gamma, Normal and Pareto) and the discrete parameter values found in the relative cluster (Old Plaster cluster). In the case shown of the thermal conductivity of the old plaster, the distribution that best represents the discrete values is the gamma distribution

The results of the sensitivity analysis usually depend more on the ranges chosen than on the probability distributions assigned [35]. Each continuous distribution is checked to ensure that it is representative with respect to discrete values.

Matrix 1 represents a single iteration of the method. For the construction of the matrix, basic (a) and auxiliary terms (b) are generated during sampling. Each row consists of all input parameters used for each simulation. The first line consists of all basic terms (k = input parameters). In each subsequent line, a single value a is replaced by an auxiliary term as shown in **Matrix 1** for a total of k+1 lines. For each simulation, the statistical indices $\chi^2_{avg,bi}$ described in **Section 2.4** are calculated as output, which consider the comparison between simulated and monitored values under the insulation and are used as objective function.

$$\begin{matrix} a_{1,r} & a_{2,r} & \dots & \dots & \dots & \dots & a_{k,r} \\ b_{1,r} & a_{2,r} & \dots & \dots & \dots & \dots & a_{k,r} \\ a_{1,r} & b_{2,r} & \dots & \dots & \dots & \dots & a_{k,r} \\ \dots & \dots & \dots & \dots & \dots & \dots & \dots \\ a_{1,r} & \dots & a_{i-2,r} & b_{i-1,r} & a_{i,r} & \dots & a_{k,r} \\ a_{1,r} & \dots & a_{i-2,r} & a_{i-1,r} & b_{i,r} & \dots & a_{k,r} \\ a_{1,r} & a_{2,r} & \dots & \dots & \dots & \dots & b_{k,r} \end{matrix}$$

Matrix 1

The elementary effect values, EE_j^i, are then calculated according to the following equation as also described in [47]:

$$EE_j^i = \frac{Y(x_i^a x_{\sim k}^a) - Y\left(x_i^b x_{\sim k}^a\right)}{x_i^a - x_i^b} \qquad \textbf{Eq. 6}$$

The values x_i^a and x_i^b indicate the reference percentile [0, 1] corresponding to the considered input value (i). For every j^{th} iteration, the term $Y(x_i^a x_{\sim k}^a)$ represents the outcome value of the simulation with the basic value for the i^{th} input parameters while $Y\left(x_i^b x_{\sim k}^a\right)$ consider the row with the substitute auxiliar value. From the identified elementary effects, the sensitivity measures μ^* and σ^2 are calculated according to the following equations:

$$\bar{\mu}_i = \frac{1}{N}\sum_{j=1}^{N} EE_i^j \quad \text{Eq. 7}$$

$$\mu_i^* = \frac{1}{N}\sum_{j=1}^{N} \left|EE_i^j\right| \quad \text{Eq. 8}$$

$$\sigma_i^2 = \frac{1}{N-1}\sum_{j=1}^{N} \left(EE_i^j - \bar{\mu}_i\right)^2 \quad \text{Eq. 9}$$

The value μ^* describe the overall influence of the input variables on the objective function (taking in account non-monotonic relationships between the parameters). The values of σ^2 give an additional information regarding the interaction effects between all parameters.

2.5.2 Parameters Selection

In hygrothermal simulation software, the physical characteristics of every material are described by its heat and moisture transport and storage functions implemented in the material files, which depend significantly on moisture content. Varying the entire function can be complex. Therefore, it is necessary to find a simplified parameter-based approach. In practice, the behavior of the functions is often summarized by significant parameters (μ_{dry}, λ_{dry}, A_w, θ_{eff}, θ_{80}). Our methodology involves varying the basic parameters and adapting the function accordingly. The approach chosen in this study represents a compromise between simplicity of implementation and provides a link to practice. Changing specific parameters allows for rescaling the hygrothermal function to which they are related. In this study, some rescaling functions implemented in Delphin software are used.

This section presents the parameters considered for the sensitivity analysis and how their variation is considered. Since the heat storage function is equally related to the values of density and specific heat capacity, both parameters have been considered as a unique parameter. Their product, denoted by C_{vol} $[KJ/(m^3K)]$, has been taken into account (also considered in [24]).

For the purpose of this study, equations have been implemented that consider the correlation of parameters to the hygrothermal transport and storage functions. **Table 2**, **Table 3**, and **Table 4**, show the rescaling equations that have been applied for each considered parameter. In addition, the graphs in the table show how the variation of each parameter affect the hygrothermal functions (a plaster from the database has been used as an example). The initial functions are represented by the red curves, the grey curves show how by varying each parameter within a plausible range the related function is changed.

Thermal Function	**Thermal Transport**		**Thermal Storage**
Parameters	$\boldsymbol{\lambda_{dry}}$ $\boldsymbol{[W/mk]}$	$\boldsymbol{\theta_{eff}}$ $\boldsymbol{[m^3/m^3]}$	$\boldsymbol{C_{vol}}$
Rescaling equation	$\boldsymbol{\lambda(\theta_l) = \lambda_{dry} + 0.56 * \theta_l}$ **Eq. 10**		$\boldsymbol{\rho, c_p}$
Example graphs	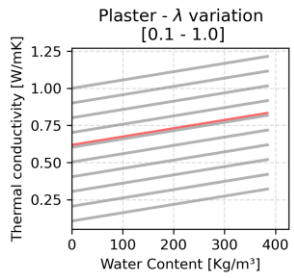	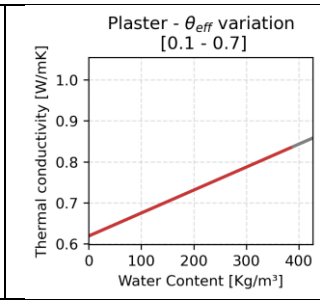	

Table 2. Rescaling functions implemented in the *Python* script to relate parameters to transport and heat storage functions.

Regarding the thermal transport, the equation in **Table 2** is used in Delphin. In particular, λ_{dry} represents the thermal conductivity of the dry material, θ_l represents its moisture content and 0.56 W/mK is the thermal conductivity of water. When λ_{dry} is varied, the function is translated but the slope remains constant. The other

changed parameter is θ_{eff} which represents the moisture content at effective saturation. This value represents the last point on the x-axis. Varying θ_{eff} extends or shortens the function.

Hygric Function	**Vapor Transport**	
Parameters	$\boldsymbol{\mu_{dry}}$ $[-]$	$\boldsymbol{\theta_{eff}}$ $[\boldsymbol{m^3/m^3}]$
Rescaling equation	$k_{v,dry}^{new} = k_{v,dry}^{old} \frac{\mu_{dry}^{old}}{\mu_{dry}^{new}}$ **Eq. 11** $\log[k_v^{new}(\theta_l)] = \log[k_v^{old}(\theta_l)] * \frac{\log[k_{v,dry}^{new}]}{\log[k_{v,dry}^{old}]}$ **Eq. 12**	$\theta_l^{new} = \theta_l^{old} \frac{\theta_{eff}^{new}}{\theta_{eff}^{old}}$ **Eq. 13**
Example graphs	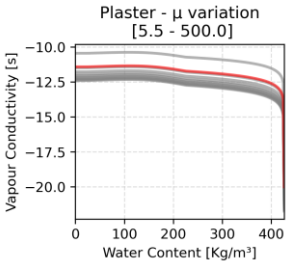	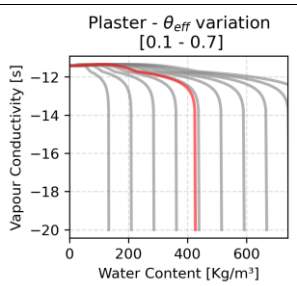

Table 3. Rescaling functions implemented in the Python script to relate parameters to vapor transport functions.

For vapor transport, a moisture content-dependent vapor conductivity (k_v) is generally implemented. **Eq. 11** and **Eq. 12** define how the function $k_v(\theta_l)$ is rescaled when the basic parameter μ_{dry} is changed from its original value (*old*) to its *new* value. **Eq. 13** shows instead the applied rescaling when the value of θ_{eff} is changed.

Hygric Function	**Liquid Transport**	
Parameters	$\boldsymbol{A_w}$ $\left[\frac{\boldsymbol{kg}}{\boldsymbol{m^2}} * \sqrt{\boldsymbol{s}}\right]$	$\boldsymbol{\theta_{eff}}$ $[\boldsymbol{m^3/m^3}]$
Rescaling equation	$k_l^{new}(\theta_{eff}) = k_l^{old}(\theta_{eff}) \left(\frac{A_w^{new}}{A_w^{old}}\right)^2$ **Eq. 14** $\log[k_l^{new}(\theta_l)] = \log[k_l^{old}(\theta_l)] * \frac{\log[k_l^{new}(\theta_{eff})]}{\log[k_l^{old}(\theta_{eff})]}$ **Eq. 15**	$\theta_l^{new} = \theta_l^{old} \frac{\theta_{eff}^{new}}{\theta_{eff}^{old}}$ **Eq. 16**
Example graphs	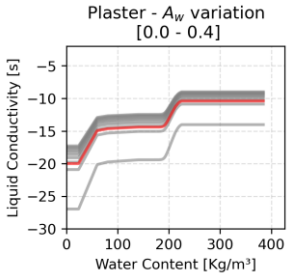	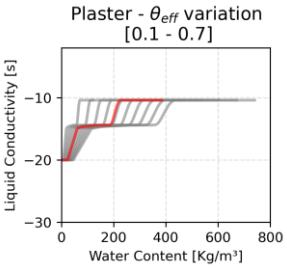

Table 4. Rescaling functions implemented in the Python script to relate parameters to liquid transport functions.

Materials in Delphin use the models for liquid water transport that considers the $k_l(\theta_l)$ (conductivity for capillary pressure gradient). **Eq. 14** and **Eq. 15** define how the function $k_l(\theta_l)$ is rescaled when the basic parameter A_w is changed from its original value (*old*) to its *new* value. **Eq. 16** shows instead the applied rescaling when the value of θ_{eff} is changed.

Hygric Function	**Moisture Storage Function**	
Parameters	$\boldsymbol{\theta_{eff}}$ $[\boldsymbol{m^3/m^3}]$	$\boldsymbol{\theta_{80}}$ $[\boldsymbol{m^3/m^3}]$
Rescaling equation	$\theta_l = \theta_{eff} * \frac{(b-1)*\varphi}{(b-\varphi)}$ **Eq. 17** $b = \varphi_{80\%} * \frac{\theta_{80} - \theta_{eff}}{(\theta_{eff} * \varphi_{80\%}) - \theta_{80}}$ **Eq. 18**	

	$\varphi_{80\%} = 0.8$ **Eq. 19**
Example graphs	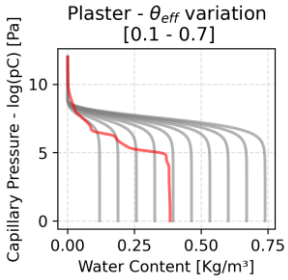 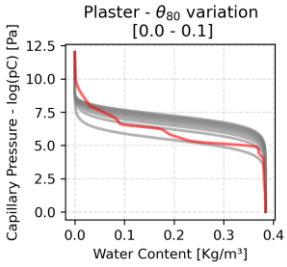

Table 5. Rescaling functions implemented in the Python script to relate parameters to moisture storage function.

The Moisture Storage Function (MSF) is defined as the moisture content of a material as a function of the relative humidity or of the capillary pressure. The MSF in Delphin is typically represented as a function of the capillary pressure allowing for a more accurate description of high moisture contents. In addition, in general, the MSF has a complex shape that depends on the pore structure of the material and is derived from different measurement points [49]. In this study, in order to simplify the sensitivity analysis methodology, the shape of the MSF is rescaled based on the variation of two basic parameters: θ_{80}, that correspond to the moisture content at a relativeθ_{eff}, that correspond to the moisture content at a relative humidity of 100%. For this purpose, the original shape of the MSF contained in the Delphin database is replaced with the analytical function described in **Eq. 17 – 19.** The graphs reported in **Table 5** show how θ_{80} and θ_{eff} affect the shape of the MSF:

The described relations are then implemented to modify the materials and perform the sensitivity analysis. The clusters identified for each type of material are considered. **Table 6** shows the probability function and the range bounds used in this study and is based on the clusters identified in the material selection phase. Note that some parameters can have a wide range of variation since the uncertainties on the materials considered in this work (described in **Section 2.3**) allowed for finding several materials which, although of the same type, can have very different parameters (e.g. λ_{dry} for the lime plaster).

Among the values obtained in the distributions and for each type of material, θ_{eff} values are almost always ten times higher than θ_{80}. However, a constraint is added in the script so that during sampling, the relation $\theta_{80} < \theta_{eff}$ is always verified.

In the calibration phase, the values of the coefficients of the boundary conditions are not varied but considered equal to the values given in the WTA recommendations and indicated in **Section 2.1**. In addition to material parameters, coupling parameters with boundary conditions are varied in the sensitivity analysis. The external and internal heat coupling coefficients (h_{ext} and h_{int}), the vapor exchange coefficients with internal and external surfaces (β_{ext} and β_{int}), the shortwave solar radiation absorption coefficient (α_{sol}), and rain exposure coefficient are all taken into account. The limits for the boundary condition coefficients are chosen based on [50]. **Tables Table** 6 and **Table** 7 show the range of variation for each material's parameter and for the coupling coefficients with the boundary conditions.

Materials/parameters	A_w		C_{vol}		λ_{dry}		μ_{dry}		θ_{eff}		θ_{80}	
	min	max	min	max	min	max	min	max	min	max	min	max
New Plaster	0.004	0.49	1277	2379	0.11	1.045	6.1	51	0.16	0.73	0.006	0.062
	Gamma		Gamma		Norm		Gamma		Gamma		Uniform	
Old Plaster	0.0001	0.367	512	1780	0.1	1	5.5	251	0.059	0.787	0.002	0.092
	Gamma		Norm		Gamma		Gamma		Gamma		Gamma	
Glue	0.0001	0.124	676	1569	0.1	1	10.3	65.0	0.059	0.787	0.002	0.092
	Gamma		Norm		Gamma		Gamma		Gamma		Gamma	
Stone	0.003	0.67	1403	1979	0.96	3.27	11	178.5	0.05	0.27	0.0007	0.036
	Gamma		Norm		Norm		Pareto		Uniform		Pareto	
Insulation	0.003	0.084	267	400	0.034	0.093	3	15	0.38	0.931	0.0176	0.0528
	Uniform		Pareto		Gamma		Pareto		Uniform		Pareto	

Table 6. Range of variation selected, and probability functions used for each material's parameter.

Parameters	α_{sol}		$Rain\ coeff.$		h_{ext}		h_{int}		β_{ext}		β_{int}	
	min	max	min	max	min	max	min	max	min	max	min	max
Variation range	0.1	1.0	0.3	1.0	12.5	50.0	3.0	15.0	1.0	17.0	1.0	5.5
Distribution	Uniform		Uniform		Uniform		Uniform		Uniform		Uniform	

Table 7. Range of variation selected for the coefficient of coupling with the boundary conditions.

3 Results and Discussions

The first step concerns the creation of material clusters, grouping material files present in the database that are representative of those present in the investigated wall. **Table 8** summarizes the number of file materials used for each cluster.

Material Type	Category	n° of materials in the cluster
New Plaster	Plaster	30
Old Plaster	Plaster	64
Insulation	Insulation	2
Glue	Plaster	32
Stone	Natural Stones	25

Table 8. Number of materials selected for every cluster.

Afterward, the identified material files are combined assigning them to the corresponding layer. An iteration procedure is conducted to find the best combination of material files that minimize the discrepancy between simulated and monitored data. For this purpose, over 4000 simulations with different material combinations are run. **Figure 7 (a)** represents the output of all simulation in terms of relative humidity under the insulation for the entire monitored period (curves in grey) in comparison with the data recorded by the sensors under the insulation (red curve with uncertainty area represented in orange). **Figure 7 (b)** shows the box plot of the values obtained considering all simulations in terms of $\chi^2_{RH,bi}$ (minimum, maximum, 1st, 2nd, 3rd, 4th quartile, mean and median).

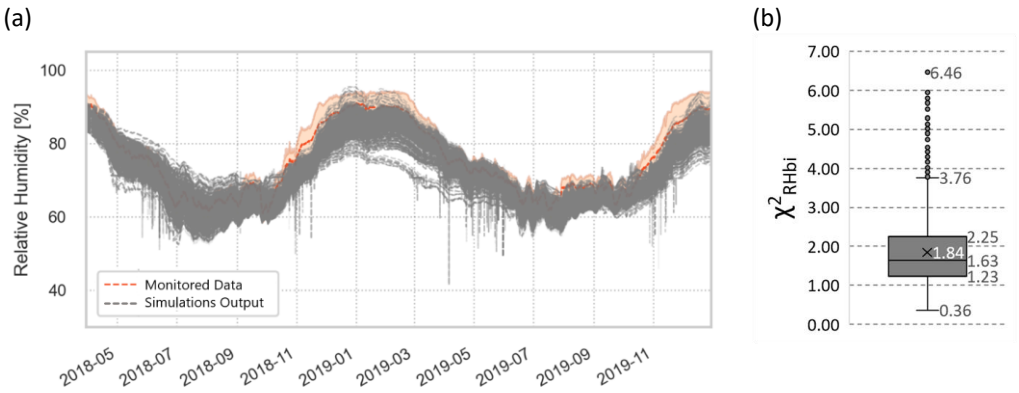

Figure 7. (a) Relative humidity between the insulation and the existing wall as a function of time is shown for the monitored data (red curve) and the different variants simulated in the calibration process. (b) Box plot representing all main values obtained in terms of $\chi^2_{RH,bi}$.

The output curves highlight the area of uncertainty that would occur if the climate data were measured, the boundary coefficients were assumed according to the WTA recommendation, and the assumed level of knowledge of the material used in this study is considered. The 75th percentile of $\chi^2_{RH,bi}$ obtained for all simulations is around 2.25 [-], while only for a few outliers, the index is higher than 3.76 [-]. All material

combinations reproduce the overall qualitative trend of the simulation. This shows that imposing the proper boundary conditions and selecting the materials carefully provides a solid basis for setting up a hygrothermal simulation model. However, from a quantitative point of view, the maximum relative humidity changes from 75% up to 95%, which is not a negligible difference when predicting moisture-related damages in constructions. Only a few curves underpredict the relative humidity curve in winter, while many of the obtained combinations are reliable.

Among all the simulations run, those that returned a very low $\chi^2_{avg,bi}$ index had the same material file for the stone. In particular, it is a sandstone existing in the province of Rüthen in Germany. Stone is a mixed material with historic mortar and other impurities, so it is the element whose properties are most uncertain. At the same time, it constitutes the thickest layer of the wall. The material identified may not be representative of stone, but it more effectively balances the characteristics of the complex wall element.

Figure 8 shows the best combination of materials obtained by the calibration process described in **Section 2.3**.

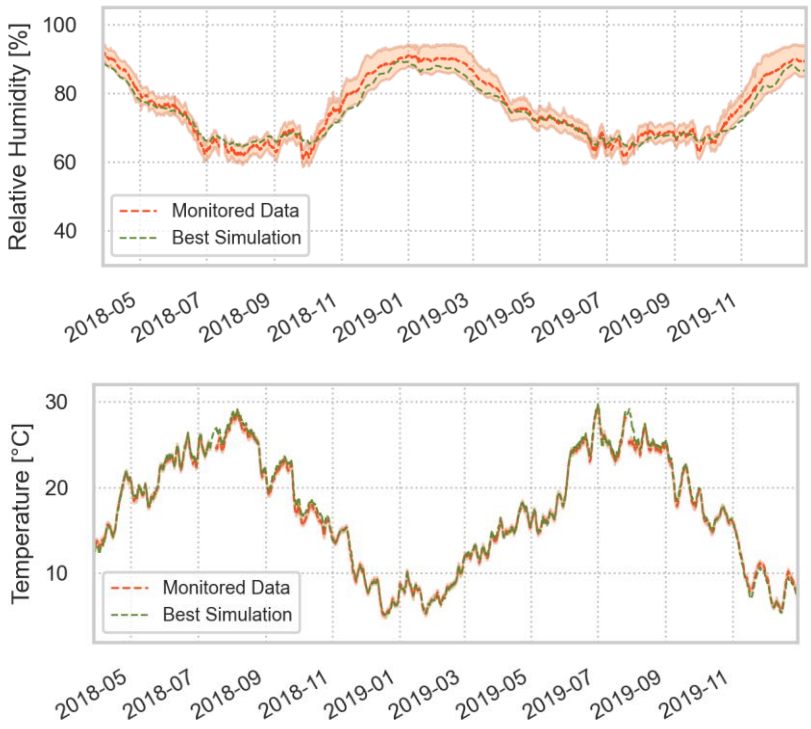

Figure 8. Output values of relative humidity and temperature behind the insulation of the simulation with the best combination of materials.

These curves represent the one with the lowest value in terms of index $\chi^2_{avg,bi}$. The calibrated model shows the relative humidity values under the insulation within the area of the uncertainty of the monitored data for almost the entire monitored period. Considering the materials in the software database (and the above-explained clusterization), a model with a $\chi^2_{RH,bi}$ of 0.43 [-] is obtained. The comparison with the temperature values at the same position returns simulation values close to those monitored, with a $\chi^2_{T,bi}$ of 4.9. To compare the results with better-known indices in the literature, **Table 9** shows the values of MAE and RMSE.

Index	RH_{bi}	T_{bi}	Hourly criteria
MAE	1.87 %	0.31 °C	<1°C (temperature)
RMSE	2.24 %	0.45 °C	< 5% (relative humidity) [21]

Table 9. MAE and RMSE values obtained for the calibrated model.

Although it is more straightforward than other approaches, the calibration with the parametric method gives a result very close to the experimental data. Moreover, past analyzes [24] have also shown that this approach provides a good calibration. In fact, in [24], it was seen that calibration with more sophisticated optimization methods (e.g. GenOpt) does not lead to consistent improvements in hygrothermal behavior. Furthermore, the same article discussed how optimization processes provide a calibrated model, but the parameters obtained do not necessarily reflect reality.

Afterward, in this work, the numerical model is validated. The calibrated simulation is compared with a later period based on the hourly relative humidity measure. **Figure 9** compares the calibrated model and the monitored relative humidity data under the Insulation from 01/01/2022 to 24/07/2022.

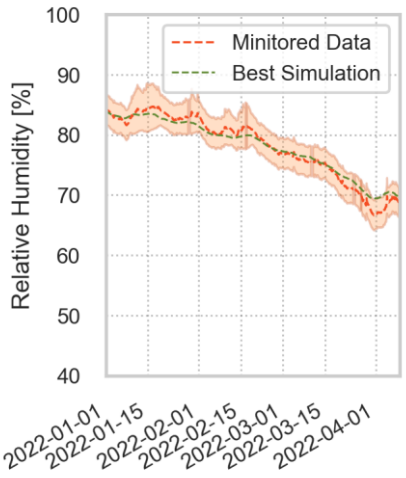

Figure 9. Comparison of simulated and monitored data carried out for validation (01/01/2022 to 24/07/2022)

The graph shows an excellent agreement between simulated and monitored data two years after model calibration. The statistical indices obtained in this period are 0.18 [-] for $\chi^2_{RH,bi}$. This indicates that the calibrated model continues to be representative for the case study analyzed.

Index	RH_{bi}	T_{bi}	Hourly criteria
MAE	0.89 %	0.39 °C	<1°C (temperature)
RMSE	1.11 %	0.52 °C	< 5% (relative humidity) [21]

Table 10. MAE and RMSE values obtained for the model validation.

As a result, can be assumed that the obtained curves are calibration of the numerical model that identifies a material file combination with properties that allow for good agreement with what is being monitored. The model's complexity and numerous uncertainties make it impossible to precisely match material parameters. Three factors must be considered:

- It is possible that the materials present in the wall do not match those in the database.
- Some material properties can be balanced and still provide an optimal result.
- Some parameters in the numerical model may have a greater influence than others. The result of the calibration for the less impactful parameters is affected by a high degree of uncertainty

This study focuses on the third point in particular. A sensitivity analysis has been performed starting from the calibrated model to identify the most influential input parameters in the hygrothermal simulation.

The sensitivity analysis results identify the parameters that significantly influence the simulation with regards to the specified objective functions. This study concentrates on the $\chi^2_{RH,bi}$ and $\chi^2_{T,bi}$ value, which

quantifies the discrepancy between the simulated and monitored relative humidity and temperature under the insulation. Starting with a calibrated model can give excellent reliability to the sensitivity analysis. The methodology is repeated, starting with different material combinations (also, those combinations have curves very close to the monitored ones). It is possible to verify whether different hygrothermal functions of different materials could affect the results. It is therefore verified that the ranking of the parameters is approximately similar even when different material combinations are applied. The sensitivity analysis results are presented in **Figures Figure** 10 **(a)** and **10 (b)**. The values of μ^* on the x-axis represent the influence of the individual parameter, while the coefficient σ^2 provides additional information about the effects of parameter interactions.

(a)

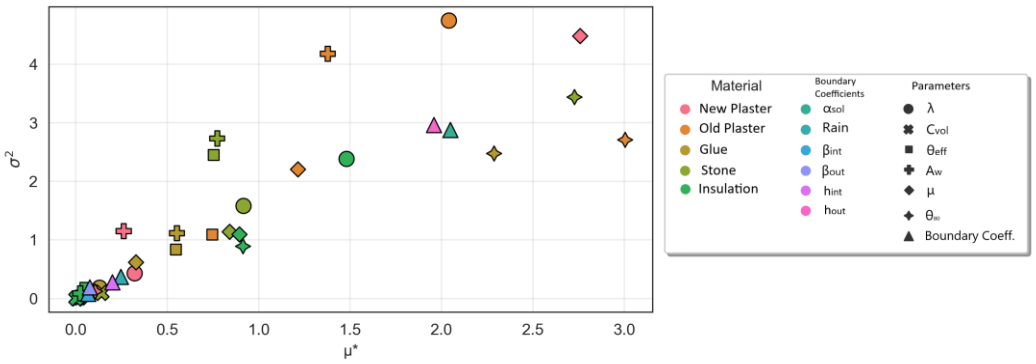

(b)

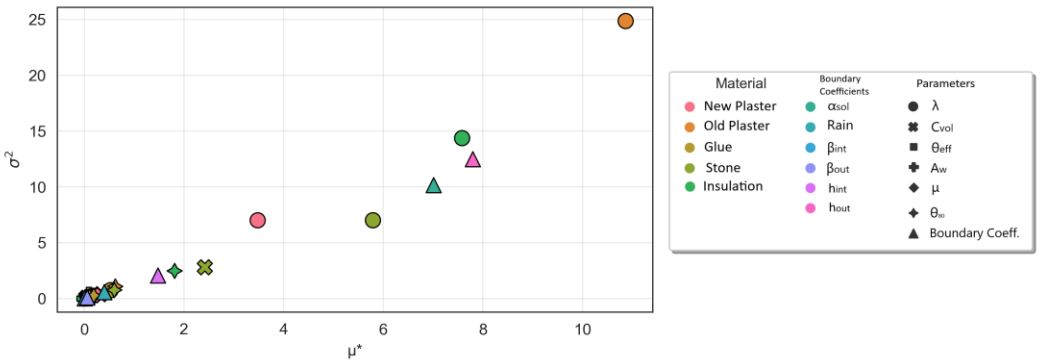

Figure 10. Sensitivity analysis results using the Morris Method considering the relative humidity **(a)** and temperature **(b)** monitored under the insulation. On the x-axis $\boldsymbol{\mu^*}$ indicate the influence of the parameter on the objextive function. On y-axis $\boldsymbol{\sigma^2}$ raperents the correlation's effect.

Table 11 summarizes the figure for a more effective representation:

Boundary Coefficients	Materials / Parameters	New Plaster	Old Plaster	Glue	Stone	Insulation		
α_{sol}	C_{vol}						$\mu^* > 3$	Very Influential
$Rain$	λ						$\mu^* > 2$	
h_{int}	θ_{eff}						$\mu^* > 1$	
h_{ext}	θ_{80}						$\mu^* > 0.5$	
β_{int}	A_w						$0 < \mu^* < 0.5$	Not influential
β_{ext}	μ							

Boundary Coefficients	Materials / Parameters	New Plaster	Old Plaster	Glue	Stone	Insulation		
α_{sol}	C_{vol}						$\mu^* > 0.40$	Very Influential
$Rain$	λ						$\mu^* > 0.30$	

h_{int}	θ_{eff}	$\mu^* > 0.20$			
h_{ext}	θ_{80}	$\mu^* > 0.10$			
β_{int}	A_w	$0 < \mu^* < 0.10$			Not influential
β_{ext}	μ				

Table 11. Summary table of $\boldsymbol{\mu}^*$ values obtained with the Morris Method for the relative humidity and temperature values

The results of the sensitivity analysis are specific to the analyzed case study. In general, they are related to three factors:

- Cross-section: The type of materials present, their thicknesses and their distribution within the wall can affect the obtained results.
- Climate conditions. The geographical location of the analyzed masonry and the surroundings (presence of other buildings or vegetation) can change the climatic conditions to which the component is exposed.
- Knowledge level. The results of the sensitivity analysis largely depend on the available information on the materials [51]. This can affect the selection of material files for the creation of the clusters. Furthermore, this has an impact on the distributions and ranges values of every considered input parameter.

Therefore, it must be underlined that, for this specific wall, in this specific climatic context and with the level of knowledge set for the materials, the authors are able to identify the most influential parameters concerning the chosen objective function (temperature and relative humidity under the insulation).

Although no work in the literature considers the value of θ_{80} among the analyzes for parameter variation, it is evident from the result that it is the one that counts most in this specific model. A possible interpretation could be that the simulation shows that the measured relative humidity in the critical point under the insulation varies from 60 % to a maximum of 90 %. This indicates that the hygroscopic state of the materials rarely reaches the over-hygroscopic range, so transport is mainly via vapor. Furthermore, θ_{80} values with the most significant impact are precisely those of the materials closest to the compared position. **Figure 11** shows the relative humidity values output obtained with the calibrated simulation. The great variability of this value in the ranges used could be the reason why this parameter is found to have a considerable influence on the results. For this reason, knowledge of this parameter could point toward the choice of representative materials.

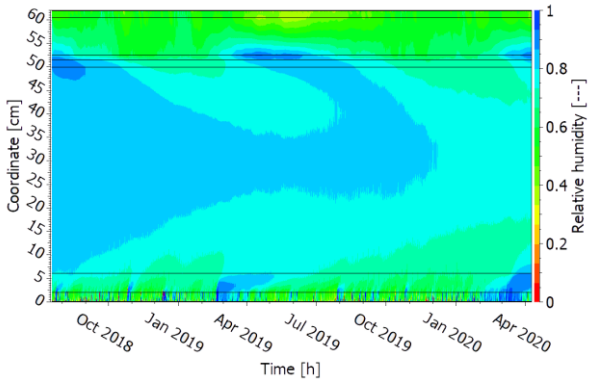

Figure 11. Representation of relative humidity values throughout the simulated period. The x-axis shows the simulated period. The left y-axis shows the thickness of the wall (in cm). The right y-axis indicates the colour scale used to represent the relative humidity values.

Thermal conductivity plays an important role in determining relative humidity and temperature within the wall, as also shown in several studies [24,26,31,52,53]. The material whose thermal conductivity affects the numerical model more, in terms of humidity and temperature under the insulation, is the *old plaster*. The interpretation of this result could be evaluated through the wall's thermal resistances of every material component. Furthermore, the position of the old plaster layers with the investigated point is essential for analyzing the result. In contrast to the *new plaster*, the two layers of *old plaster* are located to the left of the insulation (and the measured point). Therefore, the thermal resistances to be compared are those of the *stone*

layer and the *old plaster*. The graph in **Figure 12** shows that when comparing the ranges of variation considered for this study, the dominant thermal resistance regards the historic plaster. This is because a lower thermal conductivity value creates an insulating effect from the outside, which raises the temperature. As a result, the vapor pressure difference between the external layers and the insulation is lowered, reducing the vapor transport at that point. A low λ_{dry} value for historical plaster (present in the range) could, therefore, significantly influence the results in terms of relative humidity and temperature. Particularly important to note that the relative humidity behind the insulation, which is connected with the risk for interstitial condensation, depends strongly on the thermal conductivity. This parameter is usually considered negligible for the energy performance as soon as a wall is insulated and thus not investigated further.

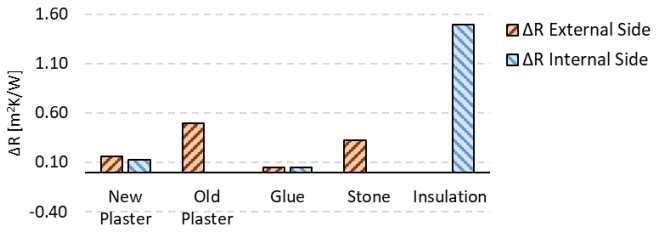

Figure 12. Comparison of the resistance difference referred to the range of variation of each material. The material layers' position refers to the monitored point under the insulation.

As shown by the work carried out by Zeng et al. in [1] water absorption coefficient of the external plaster influences long-term moisture accumulation. This is confirmed by the results of the sensitivity analysis carried out in this work. Since the plaster is applied to both the inner and outer surface, it is plausible to assume that the μ_{dry} value determines the vapor flow within the wall. In contrast, there is a narrow range of variation for the μ_{dry}-value in the case of insulation. Nonetheless, the results show a remarkable importance regarding the knowledge of this value. In general, the result shows that the coefficient μ_{dry} is an important input parameter for each material in the wall (except stone material).

Regarding the coefficients of the boundary conditions, only α_{sol} and h_{ext} are found to play a role in the influence of the objective function. A previous study carried out on the same case study considering only the thermal parameters yielded the same result [24]. In the reported study, the objective function did not refer to the moisture under the insulation but an average index that considered the temperatures in the three monitored points. Therefore, it can be stated that these parameters should be carefully set during the creation of a numerical model. The density and specific heat capacity of the materials described by the C_{vol} parameter is found to be non-influential (again confirmed in [17,24]).

A further analysis is carried out to compare the change in the relative humidity under the insulation for each individual material. Starting from the best combination (which has provided the lowest ($\chi^2_{avg,bi}$), several simulations have been run by varying one material at a time in the respective clusters. **Figure 13** shows all the curves obtained for each material file and the respective parameter values. A correlation coefficient (Pearson) is determined for each parameter by correlating its values with the objective function.

As far as the *new plaster* is concerned, the graph confirms what the Morris method reveals. There is no considerable influence from this material. The maximum difference in relative humidity is no more than 10 %. Furthermore, the only parameter that correlates with the results is μ_{dry}. A high value of μ_{dry} tends to increase the relative humidity in summer and slightly lower it in winter. This could be due to the position of the plaster covering the external and internal surfaces; a high μ_{dry}-value acts as a barrier to the boundary conditions and decreases the moisture variation in the wall. Of the three wood fiber insulators, two have a very similar trend. The third shows a significant underestimation of relative humidity. The relative humidity values in the latter case are around 60 % for the entire simulated period. Further discussion of this aspect is not covered in this article. The choice of plaster in this case study can have the greatest influence on the objective function. Confirming the

Morris method, the graphs show a correlation between the thermal conductivity value of the material and the objective function, especially in the colder months. A slight correlation (Pearson 0.6) is also present with the C_{vol} value. This can be explained by the fact that thermal conductivity is related to the density of the material. Although the glue layer is only 1 cm, it also represents the layer in which the sensors are placed. The choice of glue has little influence on the change in relative humidity, which, at worst, is less than 10 %. However, there is a slight correlation between the values of μ_{dry}. A high value of this parameter brings the simulated curve closer to the monitored one. The stone material constitutes the thickest layer of the investigated wall (44 cm). Nevertheless, the choice of different materials does not influence the hygrothermal simulation. The comparison graphs between the materials and the objective function do not clearly correlate the investigated parameters.

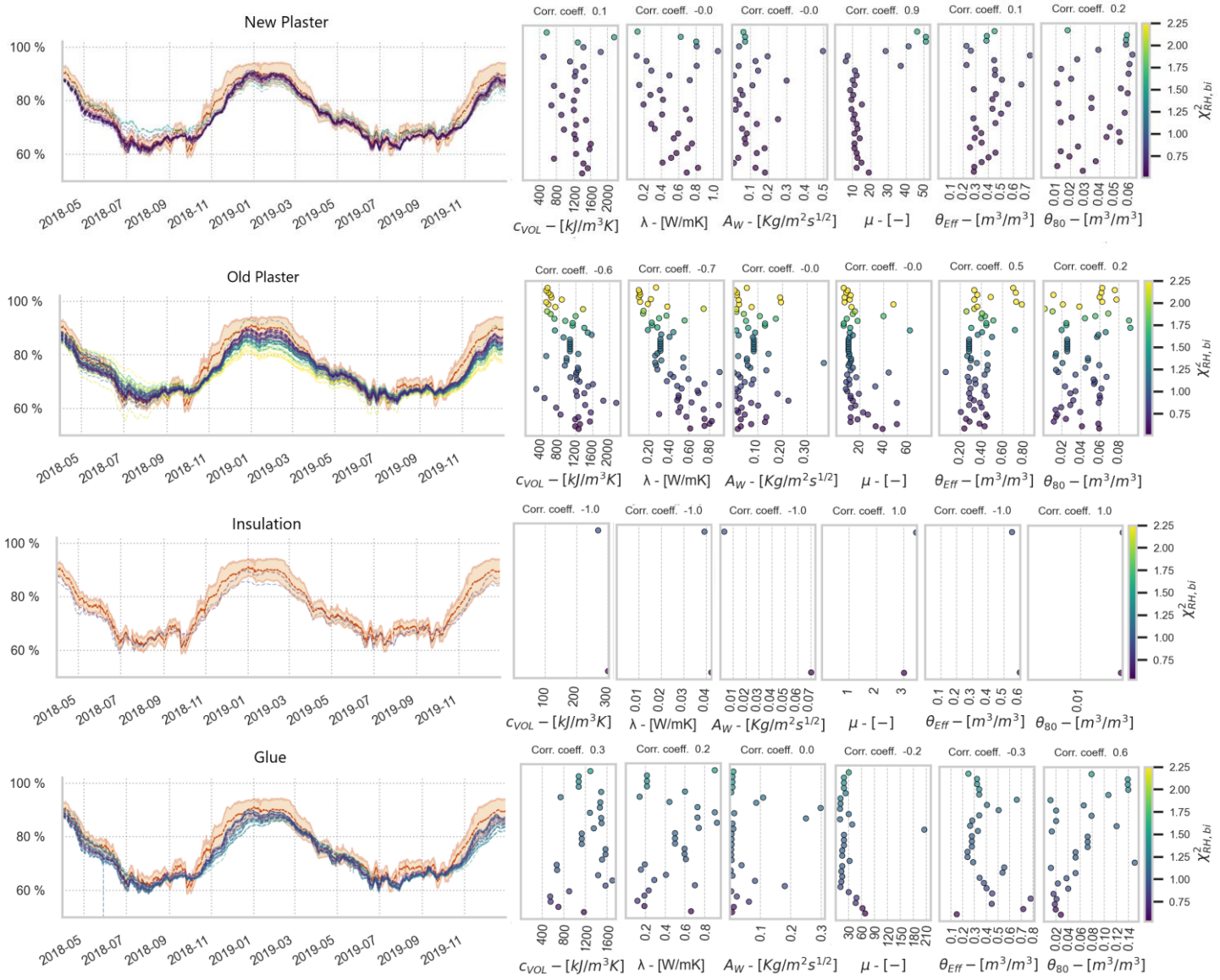

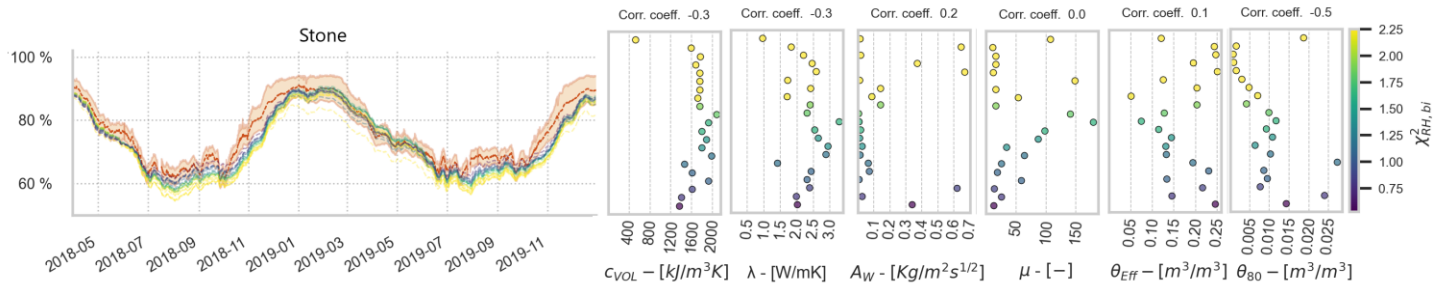

Figure 13. Comparison of the output values of the relative humidity behind the insulation obtained by starting with the best combination and varying one material at a time within each cluster. The scatter plots show the correlation between each parameter and the $\chi^2_{RH,bi}$-index value.

4 Conclusion

This paper presents a calibration and sensitivity analysis on a DELPHIN model based on a case study in Settequerce (Bolzano – Italy). The first research question concerns the reliability of the hygrothermal simulation and how far the numerical model can represent reality. A monitored system has been installed to collect data on the climate conditions (internal and external), together with temperature and relative humidity values within the cross-section. Based on this data, a methodology is implemented to find a combination of materials within the database that reduce the difference between the relative humidity values under the insulation obtained as the output of the numerical model and the values recorded by the sensors. Therefore, starting from the best combination of materials, a sensitivity analysis is carried out with the aim of finding the parameters that are the most influential in the numerical model. The methodology presented in this study aims to provide support to designers during the creation of a numerical model. Measuring the parameters that have the greatest impact in the hygrothermal simulation could help to obtain a more reliable model. Since laboratory tests can be expensive and time-consuming, knowing this information might suggest to the designers which parameters they should spend more effort on.

The results have shown that excellent agreement can be obtained between the monitored data and the simulation outcome. The relative humidity curves under the insulation obtained as output fall entirely within the area of the uncertainty of the monitored data. From analyzing all the curves obtained with all tested combinations, it can be stated that a reliable simulation could be achieved by selecting representative materials from the database of the software.

The possibility of exploiting comparison data obtained from in-situ monitoring allowed a calibrated model to be obtained, which is used for sensitivity analysis and finally validated. Due to its high computational efficiency, the Morris method has been used. It allows for the identification of relevant inputs, even when, as in this case, the model has a lot of parameters and is therefore computationally burdensome. In general, the input values referring to material parameters are more influential in comparison to the coefficients of the boundary conditions of which only h_{ext} and α_{sol} have a slight influence. In the analyzed wall, the greater uncertainty about the historical plaster combined with its position within the wall makes this material the most influential in the model. In particular, the thermal conductivity of the old plaster plays an important role. A lower lambda value makes the wall more insulated from the outside and, therefore, thus warmer. This implies a lower value of relative humidity under the insulation and, therefore, less moisture accumulation.

This methodology allowed to identify a ranking of the influence of the input parameters for the numerical model of the specific case study. It is necessary to highlight that the results depend on the case analyzed and in particular:

- The cross-section composition.
- The geographical location of the case study.

- The level of knowledge of the parameters to be provided as input to the numerical model.

However, this work proposed a robust methodology that could easily be applied to other case studies. Further results could be obtained and then categorized according to the materials found in the cross-section, the climate zone in which the building is located and the level of knowledge of the input parameters. Reproducing other results using this methodology could certainly produce useful findings for designers who use hygrothermal simulations. In particular, it could direct the designer to perform specific tests to obtain information on one input parameter. Furthermore, more studies on similar buildings could validate what has been obtained.

Nomenclature:

Parameter	*Description*	*Unit*
h_{ext}	*Heat coupling coefficients with the outside*	*[W/m²K]*
h_{int}	*Heat coupling coefficients with the inside*	*[W/m²K]*
C_{vol}	*Volumetric heat capacity*	*[kJ/m³K]*
$D_{v,air}$	*Vapor diffusivity in free air*	*[m²/s]*
$T_{i,mon}$	*Temperature recorded by the sensors*	*[°C]*
c_p	*Specific heat capacity*	*[J/kgK]*
k_l	*Liquid conductivity*	*[s]*
k_v	*Vapor conductivity*	*[s]*
p_a	*Partial air pressure in gas phase*	*[Pa]*
A_w	*Water uptake coefficient*	*[kg/m²s$^{1/2}$]*
α_{sol}	*Solar radiation absorption coefficient*	*[-]*
β_{ext}	*Vapor exchange coefficients with the outside*	*[s/m]*
β_{int}	*Vapor exchange coefficients with the inside*	*[s/m]*
θ_{eff}	*Moisture content at effective saturation*	*[m³/m³]*
θ_l	*Volumetric moisture content*	*[m³/m³]*
μ_{dry}	*Water vapor diffusion resistance factor*	*[-]*
θ_{80}	*Moisture content at a relative humidity of 80%*	*[m3/m3]*
λ_{dry}	*Thermal conductivity*	*[W/mK]*
K	*Water permeability*	*[s]*
$RH_{i,mon}$	*Relative humidity recorded by the sensors*	*[%]*
$Rain\ coeff.$	*Rain exposure coefficient*	*[-]*
T	*Temperature*	*[K]*
b	*Approximation factor*	*[-]*
g	*Gravity constant*	*[m/s²]*
j	*Mass or heat flow*	*[kg/m²s] or [W/m²]*
p_l	*Liquid (capillary) water pressure*	*[Pa]*
p_v	*Partial water vapor pressure in gas phase*	*[Pa]*
x	*Coordinate*	*[m]*
λ	*Thermal conductivity*	*[W/mK]*
ρ	*Density*	*[kg/m³]*
φ	*Relative humidity*	*[%]*

Acknowledgments: The authors would like to acknowledge the financial support for this research received through the HyLAB project, Project funded by Provincia Autonoma di Bolzano – Alto Adige.

References

[1] L. Zeng, Y. Chen, C. Cao, L. Lv, J. Gao, J. Li, C. Zhang, Influence of materials' hygric properties on the hygrothermal performance of internal thermal insulation composite systems, Energy Built Environ. (2022). https://doi.org/10.1016/J.ENBENV.2022.02.002.

[2] N.F. Jensen, S.P. Bjarløv, C. Rode, E.B. Møller, Hygrothermal assessment of four insulation systems for interior retrofitting of solid masonry walls through calibrated numerical simulations, Build. Environ. 180 (2020) 107031. https://doi.org/10.1016/j.buildenv.2020.107031.

[3] Q. Ge, M. Menendez, Extending Morris method for qualitative global sensitivity analysis of models with

dependent inputs, Reliab. Eng. Syst. Saf. Volume 162 (2017) Pages 28-39. https://doi.org/10.1016/j.ress.2017.01.010.
[4] L. Wang, H. Ge, Stochastic modelling of hygrothermal performance of highly insulated wood framed walls, Build. Environ. 146 (2018) 12–28. https://doi.org/10.1016/J.BUILDENV.2018.09.032.
[5] J.L.M. Hensen, R. Lamberts, C.O.R. Negrao, A view of energy and building performance simulation at the start of the third millennium, Energy Build. 34 (2002) 853–855. https://doi.org/10.1016/S0378-7788(02)00063-4.
[6] H.L.S.C. Hens, Combined heat, air, moisture modelling: A look back, how, of help?, Build. Environ. 91 (2015) 138–151. https://doi.org/10.1016/j.buildenv.2015.03.009.
[7] E.B. Møller, Robust internal thermal insulation of historic buildings - D2.1, (2018) 143. https://www.ribuild.eu/work-packages.
[8] F. Frasca, E. Verticchio, C. Cornaro, A.M. Siani, Performance assessment of hygrothermal modelling for diagnostics and conservation in an Italian historical church, Build. Environ. 193 (2021) 107672. https://doi.org/10.1016/J.BUILDENV.2021.107672.
[9] K. Calle, N. Van Den Bossche, Sensitivity analysis of the hygrothermal behaviour of homogeneous masonry constructions: Interior insulation, rainwater infiltration and hydrophobic treatment, J. Build. Phys. 44 (2021) 510–538. https://doi.org/10.1177/17442591211009937.
[10] D. Bottino-Leone, M. Larcher, A. Troi, J. Grunewald, Hygrothermal characterization of a fictitious homogenized porous material to describe multiphase heat and moisture transport in massive historic walls, Constr. Build. Mater. 266 (2021) 121497. https://doi.org/10.1016/j.conbuildmat.2020.121497.
[11] J. Seo, F.U. Vogdt, User-dependent hygrothermal assessment and material parameter optimization for a wood-based construction under climate conditions of South Korea, MATEC Web Conf. 282 (2019) 02076. https://doi.org/10.1051/matecconf/201928202076.
[12] T. Busser, J. Berger, A. Piot, M. Pailha, M. Woloszyn, Comparison of model numerical predictions of heat and moisture transfer in porous media with experimental observations at material and wall scales: An analysis of recent trends, Dry. Technol. 37 (2019) 1363–1395. https://doi.org/10.1080/07373937.2018.1502195.
[13] T. Kalamees, J. Vinha, Hygrothermal calculations and laboratory tests on timber-framed wall structures, Build. Environ. 38 (2003) 689–697. https://doi.org/10.1016/S0360-1323(02)00207-X.
[14] M. Birjukovs, I. Apine, A. Jakovics, Establishing material hygrothermal characteristics via long-term monitoring and best-fit numerical models, E3S Web Conf. 172 (2020) 17009. https://doi.org/10.1051/e3sconf/202017217009.
[15] K.U.J. Straube, Pe.R. Van Straaten, Field Monitoring and Simulation of a Historic Mass Masonry Building Retrofitted with Interior Insulation, in: 12th Int. Conf. Therm. Perform. Exter. Envel. Whole Build., 2013.
[16] P. Freudenberg, U. Ruisinger, E. Stöcker, Calibration of Hygrothermal Simulations by the Help of a Generic Optimization Tool, in: Energy Procedia, Elsevier Ltd, 2017: pp. 405–410. https://doi.org/10.1016/j.egypro.2017.09.645.
[17] M. Gutland, S. Bucking, M.S. Quintero, Calibration of an historic masonry building using measured temperature and heat flux data, in: Proc. Build. Simul. 2019 16th Conf. IBPSA. Build. Simul. 2019, International Building Performance Simulation Association, 2019. https://doi.org/10.26868/25222708.2019.210576.
[18] I. Costa-Carrapiço, B. Croxford, R. Raslan, J. Neila González, Hygrothermal calibration and validation of vernacular dwellings: A genetic algorithm-based optimisation methodology, J. Build. Eng. 55 (2022) 104717. https://doi.org/10.1016/J.JOBE.2022.104717.
[19] M. Ibrahim, H. Sayegh, L. Bianco, E. Wurtz, Hygrothermal performance of novel internal and external super-insulating systems: In-situ experimental study and 1D/2D numerical modeling, Appl. Therm. Eng. 150 (2019) 1306–1327. https://doi.org/10.1016/j.applthermaleng.2019.01.054.
[20] A. Sadłowska-Sałęga, J. Radoń, Feasibility and limitation of calculative determination of hygrothermal

conditions in historical buildings: Case study of st. Martin church in Wiśniowa, Build. Environ. 186 (2020). https://doi.org/10.1016/J.BUILDENV.2020.107361.
[21] H.E. Huerto-Cardenas, F. Leonforte, N. Aste, C. Del Pero, G. Evola, V. Costanzo, E. Lucchi, Validation of dynamic hygrothermal simulation models for historical buildings: State of the art, research challenges and recommendations, Build. Environ. 180 (2020) 107081. https://doi.org/10.1016/j.buildenv.2020.107081.
[22] G.B.A. Coelho, H.E. Silva, F.M.A. Henriques, Calibrated hygrothermal simulation models for historical buildings, Build. Environ. 142 (2018) 439–450. https://doi.org/10.1016/j.buildenv.2018.06.034.
[23] S. Panico, M. Larcher, A. Troi, I. Codreanu, C. Baglivo, P.M. Congedo, Hygrothermal analysis of a wall isolated from the inside: The potential of dynamic hygrothermal simulation, in: IOP Conf. Ser. Earth Environ. Sci., IOP Publishing, 2021: p. 012053. https://doi.org/10.1088/1755-1315/863/1/012053.
[24] S. Panico, M. Larcher, A. Troi, C. Baglivo, P.M. Congedo, Thermal Modeling of a Historical Building Wall: Using Long-Term Monitoring Data to Understand the Reliability and the Robustness of Numerical Simulations, Buildings. 12 (2022) 1258. https://doi.org/10.3390/BUILDINGS12081258.
[25] I. Costa, J. Neila González, R. Raslan, C. Sánchez-Guevara, Understanding the Challenges of Determining Thermal Comfort in Vernacular Dwellings: A Meta-Analysis, SSRN Electron. J. (2021). https://doi.org/10.2139/SSRN.3944617.
[26] J. Zhao, J. "Jensen" Zhang, J. Grunewald, S. Feng, A probabilistic-based method to evaluate hygrothermal performance of an internally insulated brick wall, Build. Simul. 14 (2021) 283–299. https://doi.org/10.1007/s12273-020-0702-6.
[27] F. Roberti, U.F. Oberegger, A. Gasparella, Calibrating historic building energy models to hourly indoor air and surface temperatures: Methodology and case study, Energy Build. 108 (2015) 236–243. https://doi.org/10.1016/j.enbuild.2015.09.010.
[28] T. Hansen, R.H. Peuhkuri, E.B. Møller, S.P. Bjarløv, T. Odgaard, Material characterization models and test methods for historic building materials, in: Energy Procedia, Elsevier, 2017: pp. 315–320. https://doi.org/10.1016/j.egypro.2017.09.738.
[29] L. Wang, H. Ge, Hygrothermal performance of cross-laminated timber wall assemblies: A stochastic approach, Build. Environ. 97 (2016) 11–25. https://doi.org/10.1016/J.BUILDENV.2015.11.034.
[30] E. Di Giuseppe, M. D'Orazio, G. Du, C. Favi, S. Lasvaux, G. Maracchini, P. Padey, A stochastic approach to LCA of internal insulation solutions for historic buildings, Sustain. 12 (2020). https://doi.org/10.3390/SU12041535.
[31] J. Zhao, R. Plagge, A. Nicolai, J. Grunewald, J. Zhang, Stochastic study of hygrothermal performance of a wall assembly - The influence of material properties and boundary coefficients, HVAC R Res. 17 (2011) 591–601. https://doi.org/10.1080/10789669.2011.585421.
[32] N. Grint, V. Marincioni, C.A. Elwell, Sensitivity and Uncertainty analyses on a DELPHIN model: the impact of material properties on moisture in a solid brick wall, E3S Web Conf. 172 (2020) 04006. https://doi.org/10.1051/e3sconf/202017204006.
[33] A. Nielsen, E.B. Møller, T.V. Rasmussen, E.J. de Place Hansen, Use of sensitivity analysis to evaluate hygrothermal conditions in solid brick walls with interior insulation, in: 5th Int. Build. Phys. Conf. IBPC, Kyoto, Japan, 2012: pp. 377–384.
[34] N. Grint, V. Marincioni, C.A. Elwell, Sensitivity and Uncertainty analyses on a DELPHIN model: the impact of material properties on moisture in a solid brick wall, E3S Web Conf. 172 (2020) 04006. https://doi.org/10.1051/e3sconf/202017204006.
[35] P. Heiselberg, H. Brohus, A. Hesselholt, H. Rasmussen, E. Seinre, S. Thomas, Application of sensitivity analysis in design of sustainable buildings, Renew. Energy. 34 (2009) 2030–2036. https://doi.org/10.1016/J.RENENE.2009.02.016.
[36] WTA, Simulation of heat and moisture transfer, (2014).
[37] D. V 18599-1, Energy Efficiency of Buildings – Calculation of the Net, Final and Primary Energy Demand for Heating, Cooling, Ventilation, Domestic Hot Water and Lighting – Part 1: General Balancing

Procedures, Terms, and Definitions, Zoning and Evaluation of Energy Sou, (2007).
[38] ISO 15927-3, Hygrothermal Performance of Buildings Calculation and Presentation of Climatic Data Part 3: Calculation of a Driving Rain Index for Vertical Surfaces from Hourly Wind and Rain Data, (2009).
[39] B. Moujalled, Y. Aït Oumériane, S. Moissette, M. Bart, C. Lanos, D. Samri, Experimental and numerical evaluation of the hygrothermal performance of a hemp lime concrete building: A long term case study, Build. Environ. 136 (2018) 11–27. https://doi.org/10.1016/J.BUILDENV.2018.03.025.
[40] J. Grunewald, Diffusiver und konvektiver Stoff- und En- ergietransport (Convective and diffusive mass and energy transport in capillary-porous building materials). PhD thesis. Dresden University of Technology, 1997.
[41] A. Nicolai, J. Grunewald, Delphin 5: User Manual and Program Reference, (2006).
[42] G.R. Ruiz, C.F. Bandera, Validation of Calibrated Energy Models: Common Errors, Energies 2017, Vol. 10, Page 1587. 10 (2017) 1587. https://doi.org/10.3390/EN10101587.
[43] A. Brambilla, T. Lea, L. Grealy, A. Kuru, Climate change and Indigenous housing performance in Australia: A modelling study, Energy Build. 273 (2022) 112399. https://doi.org/10.1016/J.ENBUILD.2022.112399.
[44] A. Saltelli, S. Tarantola, F. Campolongo, M. Ratto, Sensitivity Analysis in Practice : A Guide to Assessing Scientific Models, Joint Rese, John Wiey & Sons, Ltd, Ispra, Italy, 2004.
[45] M.D. Morris, Factorial sampling plans for preliminary computational experiments, Technometrics. 33 (1991) 161–174. https://doi.org/10.1080/00401706.1991.10484804.
[46] F. Campolongo, J. Cariboni, A. Saltelli, An effective screening design for sensitivity analysis of large models, Environ. Model. Softw. 22 (2007) 1509–1518. https://doi.org/10.1016/J.ENVSOFT.2006.10.004.
[47] F. Campolongo, A. Saltelli, J. Cariboni, From screening to quantitative sensitivity analysis. A unified approach, Comput. Phys. Commun. 182 (2011) 978–988. https://doi.org/10.1016/j.cpc.2010.12.039.
[48] M.D. McKay, R.J. Beckman, W.J. Conover, Comparison of Three Methods for Selecting Values of Input Variables in the Analysis of Output from a Computer Code, Technometrics. 21 (2012) 239–245. https://doi.org/10.1080/00401706.1979.10489755.
[49] G.A. Scheffler, R. Plagge, A whole range hygric material model: Modelling liquid and vapour transport properties in porous media, Int. J. Heat Mass Transf. 53 (2009) 286–296. https://doi.org/10.1016/j.ijheatmasstransfer.2009.09.030.
[50] V. Marincioni, G. Marra, H. Altamirano-Medina, Development of predictive models for the probabilistic moisture risk assessment of internal wall insulation, Build. Environ. 137 (2018) 257–267. https://doi.org/10.1016/j.buildenv.2018.04.001.
[51] R. Pernetti, A. Prada, P. Baggio, On the influence of several parameters in energy model calibration: The case of a historical building, in: Build. Simul. Appl., 2013: pp. 263–272. https://iris.unitn.it/handle/11572/225490#.YVq-wppByUk (accessed February 21, 2021).
[52] S.O. Mundt-Petersen, L.E. Harderup, Predicting hygrothermal performance in cold roofs using a 1D transient heat and moisture calculation tool, Build. Environ. 90 (2015) 215–231. https://doi.org/10.1016/j.buildenv.2015.04.004.
[53] M.Y. Ferroukhi, R. Belarbi, K. Limam, A. Si Larbi, A. Nouviaire, Assessment of the effects of temperature and moisture content on the hygrothermal transport and storage properties of porous building materials, Heat Mass Transf. Und Stoffuebertragung. 55 (2019) 1607–1617. https://doi.org/10.1007/S00231-018-02550-5.